THE LOCAL EFFECT OF INTERMITTENCY ON THE INERTIAL SUBRANGE ENERGY SPECTRUM OF THE ATMOSPHERIC SURFACE LAYER

JOZSEF SZILAGYI[1], GABRIEL G. KATUL[2], MARC B. PARLANGE, JOHN D. ALBERTSON[1] and ANTHONY T. CAHILL[1]
[1]*Hydrologic Science, University of California, Davis, California, 95616;* [2]*School of the Environment, Duke University, Durham, North Carolina, 27708, U.S.A.*

(Received in final form 23 October 1995)

Abstract. Orthonormal wavelet expansions are applied to atmospheric surface layer velocity measurements. The effect of intermittent events on the energy spectrum of the inertial subrange is investigated through analysis of wavelet coefficients. The local nature of the orthonormal wavelet transform in physical space makes it possible to identify a relationship between the inertial subrange slope of the local wavelet spectrum and a simple indicator (i.e. the local variance of the signal) of local intermittency buildup. The slope of the local wavelet energy spectrum in the inertial subrange is shown to be sensitive to the presence of intermittent events. During well developed intermittent events (coherent structures), the slope of the energy spectrum is somewhat steeper than $-5/3$, while in less active regions the slope is found to be flatter than $-5/3$. When the slopes of local wavelet spectra are ensemble averaged, a slope of $-5/3$ is recovered for the inertial subrange.

1. Introduction

During the past three decades, following the publication of Kolmogorov's refined similarity hypothesis in 1962, many studies have focused on the effect of intermittency on scaling laws in fully developed turbulence. A brief, general review of this research can be found in Mahrt and Howell (1994). Praskovsky and Oncley (1994), using a large number of atmospheric data sets, examined the effects of intermittency on the correlation function of energy dissipation and the energy spectrum of the longitudinal velocity component. While a correction in case of the correlation function has been reconfirmed experimentally (e.g. see Anselmet *et al.*, 1984; Praskovsky and Oncley, 1994; Katul *et al.*, 1994), no measurable deviation from the $-5/3$ exponent in the inertial subrange spectrum was found. Since intermittency affects significantly the structure functions, it must have an impact on the slope of the energy spectrum too (although not necessarily in the inertial subrange); however, this latter case has not been confirmed by experiments. One explanation may be that generally this effect is too small for adequate identification in spectra (e.g. Praskovsky and Oncley, 1994; Mahrt and Howell, 1994).

This paper focuses on the slope of the inertial subrange energy spectrum of streamwise atmospheric surface layer (ASL) velocities using discrete orthonormal wavelet transforms. The turbulence in the ASL is ideal for investigating Kolmogorov's original theory (1941, hereafter referred to as K41) and intermittency

Boundary-Layer Meteorology **79:** 35–50, 1996.

effects on K41, since the Reynolds number is typically very high and, accordingly, the scale of separation between the integral length scale (L) and the Kolmogorov microscale (η) is large ($L/\eta \approx 10^6$ for ASL turbulent flows).

The use of wavelet transforms to investigate local exponents within the inertial subrange was carried out by Bacry *et al.* (1991) using wind-tunnel velocity measurements. Applying a continuous wavelet transform (Mexican hat wavelet), they found that the local scaling exponents of the velocity difference between two points vary between −0.5 to 1.0 with a mean of 0.33. They attributed this high variability in the local exponents to intermittency build up.

The application of wavelet transforms rather than Fourier transforms in this study is justified by the following considerations. If intermittency has an effect on the energy spectrum slope (which could be expected due to its proven effect on the correlation functions), then this effect should also depend on some measure of intermittency of the flow under investigation. Since turbulent intermittent events, by definition, are localized in space and time, it is natural to construct an analysis which is also localized in space (time). The wavelet transform is an obvious choice, since the wavelet coefficients at different scales are also localized, making it possible to derive local characteristics of the flow based on these coefficients. The Fourier spectrum is well localized in the frequency domain, but non-local in physical space. It can only be made local in physical space by chopping up the original signal into small segments with the help of a window function and applying Fourier transforms repeatedly on the separate or overlapping windowed segments (short-time Fourier transform) (e.g. see Cohen, 1995). We note that the structure function offers similarly smooth inertial range scaling (Albertson *et al.*, 1995). However, a final and unique benefit of the wavelet transform is that its spatially distributed coefficients can also serve as a measure of local intermittency buildup.

2. Wavelet Transforms and Spectra

Here, for completeness, a brief overview of wavelet transforms and wavelet spectra is presented. Much of this material is discussed further in Katul *et al.* (1994).

2.1. Wavelet transforms

Wavelet transforms allow the decomposition of a signal into space and scale. While there are many types of wavelet transforms, they can all be classified as either continuous or discrete. Daubechies (1992) further classified the discrete wavelet transforms as either redundant discrete systems (also known as frames) or orthonormal wavelet expansions. Continuous wavelet transforms were introduced by Grossmann and Morlet (1984, 1985) and have been applied often to turbulence (e.g. Argoul *et al.*, 1989; Everson *et al.*, 1990; Liandrat and Moret-Bailly, 1990; Farge, 1992a,b). Discrete wavelet transforms constructed from orthonormal wavelets (e.g.

Daubechies, 1988; Mallat, 198
applied to turbulence by various
and Hagelberg, 1993; Gao and L
1994a,b; Mahrt and Howell, 199
orthonormal wavelet expansion
a complete orthonormal basis,
overcomplete basis which can
wavelet coefficients (Yamada a
Kumar and Foufoula-Georgiou,
signal information; that is, a disc
N wavelet coefficients, while in
N^2 coefficients. Due to these pr
were applied in our analysis.

Daubechies (1988, 1992) anc
form spacing for the scale discret
at larger scales allows a complete
basis functions are defined by

$$F_{[j]}^{(m)}(x) = a_0^{-m/2} F\left(\frac{x - jb}{a_0^m}\right.$$

where m and j are scale and po
dilation, and b_0 is the translatio
efficient case for practical com
$a_0 = 2$ and $b_0 = 1$ (Daubechies
and translations along $2^m j$ contr

$$f(j) = \sum_{m=-\infty}^{\infty} \sum_{i=-\infty}^{\infty} w^{(m)}[i] g$$

where $g^{(m)}[i]$ is a discrete versio
discrete function $g^{(m)}[i]$ satisfies

$$\sum_{k=-\infty}^{\infty} g^{(m)}[k - 2^m j] g^{(n)}[k -$$

where δ_{ij} is the Kronecker delta.
m and position index i can be ob

$$w^{(m)}[i] = \sum_{j=-\infty}^{\infty} g^{(m)}[j - 2^m i$$

Daubechies, 1988; Mallat, 1989a,b; Meneveau, 1991a,b; Mahrt, 1991) have been applied to turbulence by various authors (e.g. Gamage and Blumen, 1993; Gamage and Hagelberg, 1993; Gao and Li, 1993; Hagelberg and Gamage, 1994; Katul *et al.*, 1994a,b; Mahrt and Howell, 1994; Turner and Leclerc, 1994; Qiu *et al.*, 1995). The orthonormal wavelet expansion differs from the continuous case in that it forms a complete orthonormal basis, while the continuous wavelet transform forms an overcomplete basis which can bring about undesired relationships between the wavelet coefficients (Yamada and Ohkitani, 1990, 1991a,b; Meneveau, 1991a; Kumar and Foufoula-Georgiou, 1993). Orthonormal wavelet expansions conserve signal information; that is, a discretely sampled turbulent signal at N points yields N wavelet coefficients, while in the continuous case, the transform can yield up to N^2 coefficients. Due to these properties discrete orthonormal wavelet transforms were applied in our analysis.

Daubechies (1988, 1992) and Mallat (1989a,b) showed that a logarithmic uniform spacing for the scale discretization with increasingly coarser spatial resolution at larger scales allows a complete orthogonal wavelet basis to be constructed. These basis functions are defined by

$$F_{[j]}^{(m)}(x) = a_0^{-m/2} F\left(\frac{x - jb_0a_0^m}{a_0^m}\right), \tag{1}$$

where m and j are scale and position indexes, respectively, a_0 is the base of the dilation, and b_0 is the translation length in units of a_0^m. The simplest and most efficient case for practical computations is the dyadic arrangement resulting in $a_0 = 2$ and $b_0 = 1$ (Daubechies, 1992; Chui, 1992). All scales along octaves 2^m and translations along $2^m j$ contribute to the construction of $f(x_j) = f(j)$ using

$$f(j) = \sum_{m=-\infty}^{\infty} \sum_{i=-\infty}^{\infty} w^{(m)}[i] g^{(m)}[i - 2^m j], \tag{2}$$

where $g^{(m)}[i]$ is a discrete version of the continuous wavelet $F(x)$ at scale m. The discrete function $g^{(m)}[i]$ satisfies the orthogonality condition

$$\sum_{k=-\infty}^{\infty} g^{(m)}[k - 2^m j] g^{(n)}[k - 2^n j] = \delta_{ij}\delta_{mn}, \tag{3}$$

where δ_{ij} is the Kronecker delta. The discrete wavelet coefficients at scale index m and position index i can be obtained by the following convolution

$$w^{(m)}[i] = \sum_{j=-\infty}^{\infty} g^{(m)}[i - 2^m j] f[j], \tag{4}$$

and they satisfy the conservation of energy condition

$$\sum_{j=-\infty}^{\infty} f[j]^2 = \sum_{m=-\infty}^{\infty} \sum_{i=-\infty}^{\infty} (w^{(m)}[i])^2, \tag{5}$$

which is similar to Parseval's identity in Fourier series (Chui, 1992). In general, the number of observations is finite and the summations in the above equations do not extend to infinity. If $N = 2^M$ is the number of observations, then (5) is written in practice as

$$\sum_{j=1}^{N} f[j]^2 = w_0^2 + \sum_{m=1}^{M} \sum_{i=1}^{2^{M-m}} (w^{(m)}[i])^2, \tag{6}$$

where the coefficient w_0^2 is zero if the function f has a zero mean. Note that with increasing scales the spatial resolution becomes coarser (e.g. at $m = 1$, we have $N/2$ coefficients, at $m = 2$ we have $N/4$ coefficients, and finally at $m = M$ we have 1 coefficient). This dyadic arrangement is suitable for turbulence studies since the small-scale features of the turbulent flow, which can change rapidly compared to the large-scale features, are characterized by the highest number of wavelet coefficients.

2.2. WAVELET SPECTRA

In Fourier analysis the power spectral density function $E(k)$ represents the energy density contained in the wavenumber bandwidth dk, spaced linearly and centered. In contrast, in the case of wavelet spectra, that information is obtained only on octaves 2^m ($m = 1, \ldots, \log_2(N)$, where N is the number of observations). For normalization purposes, and for comparisons with Fourier transforms, the time average is subtracted from the original signal so that each signal has a zero mean value. In addition, it is assumed that the observations are sampled every dy ($= \langle u \rangle / f_s$, where $\langle u \rangle$ is the mean horizontal velocity, f_s is sampling frequency) metres instead of a unit length. The variance of the signal, in terms of the wavelet coefficients, is deduced from (6) using

$$\sigma^2 = N^{-1} \sum_{m=1}^{M} \sum_{i=1}^{2^{M-m}} (w^{(m)}[i])^2, \tag{7}$$

where N is the number of observations (a power of 2), M is $\log_2(N)$, m is the scale index, and i is the position index. The total energy $T_E^{(m)}$ contained in scale $R_m = 2^m dy$ is given by

$$T_E^{(m)} = N^{-1} \sum_{i=1}^{2^{M-m}} (w^{(m)}[i])^2. \tag{8}$$

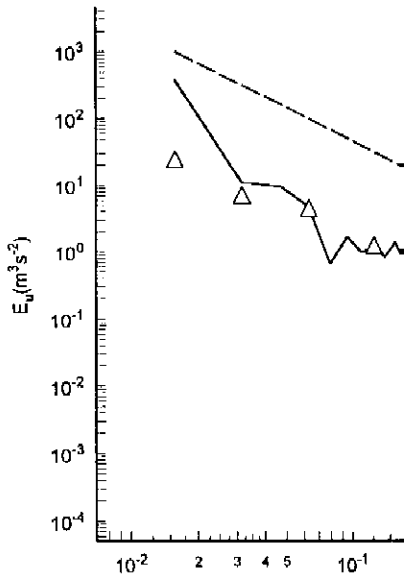

Figure 1. Fourier and wavelet spectr

The wavenumber corresponding to

$$k_m = \frac{2\pi}{R_m}.$$

The power spectral density functio
Δk_m, which is given exactly by

$$\Delta k_m = \frac{2\pi}{2^m dy} = k_m.$$

Thus the spectral density can be ex

$$E(k_m) = \langle (w^{(m)}[i])^2 \rangle \frac{dy}{2\pi},$$

where $\langle . \rangle$ is the averaging in space c
expression is different from that of
applied a Taylor series expansion t
Δk_m can be derived directly (10), w
see Appendix. For a sample wavele

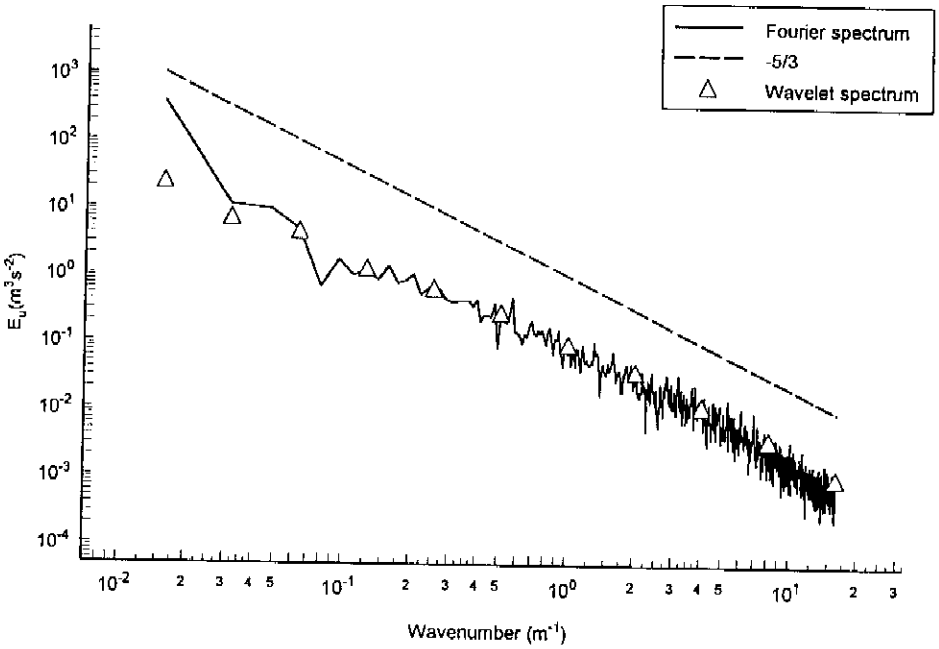

Figure 1. Fourier and wavelet spectra of a sample 20 min longitudinal velocity data file.

The wavenumber corresponding to scale R_m is

$$k_m = \frac{2\pi}{R_m}. \tag{9}$$

The power spectral density function is (8) divided by the change in wavenumber Δk_m, which is given exactly by

$$\Delta k_m = \frac{2\pi}{2^m dy} = k_m. \tag{10}$$

Thus the spectral density can be expressed the following way

$$E(k_m) = \langle (w^{(m)}[i])^2 \rangle \frac{dy}{2\pi}, \tag{11}$$

where $\langle . \rangle$ is the averaging in space over all values of i (see Meneveau, 1991a). This expression is different from that of Meneveau (1991a) and Katul *et al.* (1994), who applied a Taylor serics expansion to (9) and retained the first term only. However, Δk_m can be derived directly (10), without resort to an expansion. For the derivation see Appendix. For a sample wavelet and Fourier spectrum see Figure 1.

3. Experiment

The measurements were carried out on July 15 and 16, 1995 at 5.2 m above the ground surface over an *Alta fescue* grass site at the Blackwood division of the Duke Forest in Durham, North Carolina which is in a transition zone between the coastal plain and the Piedmont plateau. The site is a 480 m by 305 m grass-covered forest clearing (site elevation = 163 m; latitude = 35°58′ N; longitude = 79°8′ W). The mean grass height was 45 cm during this experiment. A triaxial ultrasonic anemometer (Gill Instruments 1012R2) was used to log the three velocity components, at f_s = 56 Hz, for z = 5.2 m above the local surface. The ultrasonic anemometer was mounted on a 12 m mast, situated at 250 m and 160 m from the north and west edges of a 12 m Loblolly pine forest. The closest point of the horizontal arm of the mast was at least 80 cm below the center of the measurement volume. The supporting 12 m vertical mast was downwind of the instrument. The distortion effect of the instrument was corrected in accordance with the manufacturer's calibration tables. Sonic anemometers achieve their frequency response by sensing the effect of wind on transit times of sound pulses travelling in opposite directions across a known path length d_{sl} (= 0.149 m for the Gill sonic anemometer). The sonic anemometer is suited for these experiments since it is free of calibration nonlinearities and atmospheric contamination drifts. The main disadvantage of sonic anemometers is typically attributed to the wavenumber distortion due to averaging over d_{sl}. This distortion is generally restricted to wavenumbers larger than d_{sl}^{-1} (= 6.67 m $^{-1}$), as discussed in Wyngaard (1981), Friehe (1986), and Kaimal and Finnigan (1994).

The experiment began at 0800 local time on both days. The 3D sonic sampled the velocity components continuously each day, with the signals written to a new file each 20 minutes (i.e. ≈65,536 (= 2^{16}) points in each file). The short sampling period was necessary to achieve quasi-steady mean meteorological conditions. A summary of the mean meteorological conditions is presented in Table I.

For analysis both the longitudinal and vertical wind components were used. In order to get proper values for the longitudinal component a coordinate rotation was applied to the measured data in a way that for each 20 minute data set the mean of the transverse velocity components equals zero.

During the analysis, Taylor's (1938) hypothesis was employed to convert time increments to space increments (Lumley, 1965; Tennekes and Lumley, 1972; Powell and Elderkin, 1974; Wyngaard and Clifford, 1977; Stull, 1988). At each data segment the slope calculation of the energy spectrum was restricted to wavenumbers that fell between $K_{\min}[= \pi z^{-1} = 0.6\ \mathrm{m}^{-1}]$ and $K_{\max}[= d_{sl}^{-1} = 6.67\ \mathrm{m}^{-1}]$.

Summary of meteorologi-
during data collection

Date of measurements (
Meteorological conditio
Mean horizontal wind s
Mean air temperature (°
Turbulence conditions:
Friction velocity (m s^{-1}
Standard deviation of hc
Standard deviation of ve
Atmosphere stability co
Measurement height (m)
Obukhov length (m)
Surface roughness:
Momentum roughness le

In the following analysis we cons
slope of the longitudinal and vert
(hereafter simply referred to as
effect on the spectrum may gene
are well localized in space and tir
locally (in physical space). To qu
of a time series of velocity measu

It is known that intermittent, c
scale halfplane of discrete wavel
cient values (see Meneveau, 199
Hagelberg and Gamage, 1994; I
one can compare the prevalence
turbulent signal, by simply avera
scales in each segment (window
higher the value is relative to a s
higher the probability is that inte
segment. In this way, one can rela
prevalence is quantified by the m
segment) to the slope of the energ
data. Note that the average of the
the variance of the original signal

Table I

Summary of meteorological, turbulence, and surface roughness conditions during data collection

Date of measurements (1995)	July 15	July 16
Meteorological conditions:		
Mean horizontal wind speed (m s^{-1})	2.13	1.94
Mean air temperature (°C)	32.8	32.1
Turbulence conditions:		
Friction velocity (m s^{-1})	0.17	0.18
Standard deviation of horizontal velocity (m s^{-1})	0.73	0.64
Standard deviation of vertical velocity (m s^{-1})	0.38	0.35
Atmosphere stability conditions:		
Measurement height (m)	5.2	5.2
Obukhov length (m)	−27.2	−23.1
Surface roughness:		
Momentum roughness length (cm)	10	10

4. Data Analysis

In the following analysis we consider how the intermittency of turbulence affects the slope of the longitudinal and vertical velocity energy spectra in the inertial subrange (hereafter simply referred to as spectra). As mentioned earlier, the intermittency effect on the spectrum may generally be small. However, since intermittent events are well localized in space and time they may have an effect on the energy spectrum locally (in physical space). To quantify how strong the intermittency is in any part of a time series of velocity measurements, an indicator function can be constructed.

It is known that intermittent, coherent events manifest themselves in the space-scale halfplane of discrete wavelet coefficients as areas with relatively high coefficient values (see Meneveau, 1991a; Turner *et al.*, 1994; Turner and Leclerc, 1994; Hagelberg and Gamage, 1994; Mahrt and Howell, 1994). Utilizing this feature, one can compare the prevalence of intermittent events in different segments of a turbulent signal, by simply averaging the squared wavelet coefficients found at all scales in each segment (window) of the data. It is assumed, in general, that the higher the value is relative to a similar value computed over the entire signal, the higher the probability is that intermittent events are present in the particular data segment. In this way, one can relate intermittent events in each segment (of which prevalence is quantified by the mean of all the squared wavelet coefficients in the segment) to the slope of the energy spectrum derived for the same segment of the data. Note that the average of the squared wavelet coefficients within a window is the variance of the original signal inside the window according to Equation (7).

The wavelet spectra for each arbitrarily long data segment can simply be calculated using Equation (11). Throughout the analysis, the wavelet coefficients were calculated using the algorithm given by Newland (1994). The Daubechies-type orthonormal wavelets were selected due to their optimal combination between wavelet length and vanishing moments. These wavelets have the maximum vanishing moments per wavelet support length. During the analysis a Daubechies wavelet with 4 vanishing moments was chosen since this wavelet has good localization in both domains: space and scale (Daubechies, 1992). Such space-scale localization is necessary to quantify the influence of localized events on the power spectrum. Furthermore, as shown by Meneveau (1991a) and Katul and Parlange (1994), the choice of the Daubechies wavelet is not critical for quantifying power laws within the inertial subrange.

The slope of the spectrum for both cases (Fourier and wavelet spectrum) can be calculated using the technique of logarithmic derivatives (Praskovsky *et al.*, 1993; Praskovsky and Oncley, 1994)

$$sl = \frac{1}{(nk-1)} \sum_{k=K_{\min}}^{K_{\max}-1} \frac{\ln[E(k+1)] - \ln[E(k)]}{\ln(k+1) - \ln(k)}, \tag{12}$$

where sl is the slope of the energy spectrum; nk is the number of k, the wavenumbers considered in the calculation; $E(k)$ is the value of the spectrum at wavenumber k, k having a minimum wavenumber value $K_{\min}[> \pi z^{-1}]$ and a maximum one $K_{\max}[\leq d_{sl}^{-1}]$.

With the mean value of the squared wavelet coefficients for each data segment (i.e. the variance of the data within the segment) as a measure of the degree of intermittency in the data window, and a numerical value for the slope of the wavelet spectrum for each window obtained from (12), one can check whether intermittency has an effect on the slope, by plotting the two values against each other. The length of the window (l) is important. If we choose a window size many times larger than the average size of coherent structures present in an intermittent flow, then intermittency effects will be evenly distributed between the windows. However, as the window length is reduced, the variance is going to have a much larger range, as the size of the window approaches that of the intermittent events. Naturally, there is a limit for decreasing the window size. When it is set too small, the number of scales present in each window (as well as the number of wavelet coefficients) becomes very small, resulting in high overall variance in the values of the calculated slopes due to the very limited $E(k)$ numbers used in (12). In order to reduce the resulting range of the slope values it is desirable to keep as many $E(k)$ values as possible which of course reduces the desired broad range in the variance values as well. As a trade off, a window size of 2,048 ($= 2^{11}$) data points was used in this analysis. Then, for the calculations of the variance there are 11 scales, while for the slope calculations of the wavelet spectra there are typically 3–4 $E(k)$

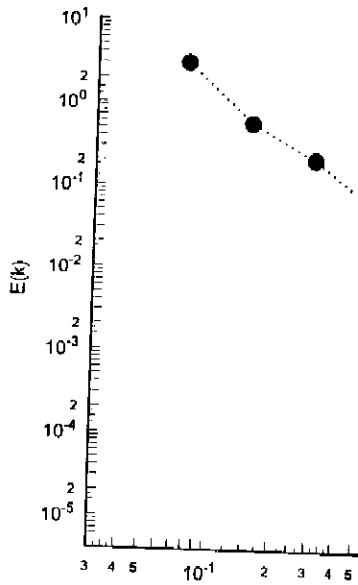

Figure 2. A sample wavelet spectrum
spectrum for each window is calculated f

values, depending on $\langle u \rangle$ inside
window ($l = 2,048$) is presented

When applying Equation (12)
wavenumber values only within
of this work is to investigate whe
spectrum). A necessary condition
isotropy, as evidenced by a ratio of
velocity energy content of 4/3 (Kai
that the wavenumber range used
subrange.

By using data windows with 2,0
20 minute file. The measurements
9 files, 20 minutes in length each,
mean and fluctuating component co
of trends), and where the slopes of
20 minute data in one window resu
calculation of sl versus the variance
altogether in $9 \times 32 = 288$ data wi
velocities. Since the variance and m
necessary to normalize the data (sub
deviation) before applying wavelet

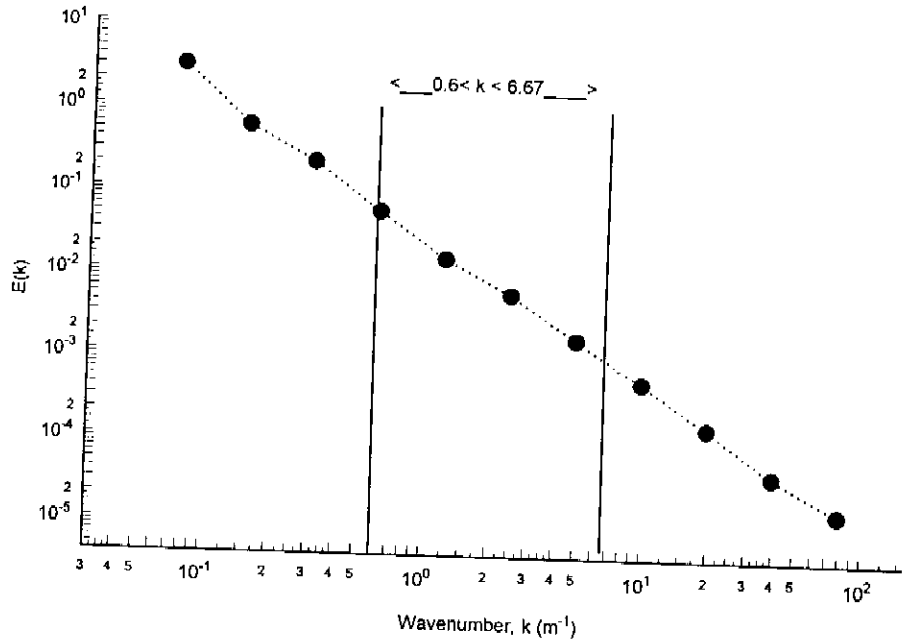

Figure 2. A sample wavelet spectrum for window length of 2,048 datapoints. The slope of the spectrum for each window is calculated for wavenumbers $0.6 < k < 6.67\ \mathrm{m}^{-1}$.

values, depending on $\langle u \rangle$ inside each window. A typical wavelet spectrum for a window ($l = 2,048$) is presented in Figure 2.

When applying Equation (12), one has to make sure to include energy and wavenumber values only within the inertial subrange scale (since the objective of this work is to investigate whether intermittency affects the inertial subrange spectrum). A necessary condition for an inertial subrange is the presence of local isotropy, as evidenced by a ratio of vertical velocity energy content to longitudinal velocity energy content of 4/3 (Kaimal and Finnigan, 1994, p. 36). Figure 3 suggests that the wavenumber range used for the analysis is in fact inside the inertial subrange.

By using data windows with 2,048 datapoints, one obtains 32 windows for each 20 minute file. The measurements conducted using 2 different days resulted in 9 files, 20 minutes in length each, where the decomposition of the signal into a mean and fluctuating component could be performed unambiguously (i.e. absence of trends), and where the slopes of the energy spectra calculated having the entire 20 minute data in one window resulted in slopes equal to $-5/3 \pm 0.01$. Thus, the calculation of $s/$ versus the variance of the signal within the window was performed altogether in $9 \times 32 = 288$ data windows for each of the longitudinal and vertical velocities. Since the variance and mean for each 20 minute data file is different, it is necessary to normalize the data (subtracting the mean and dividing by the standard deviation) before applying wavelet transforms, in order to be able to match the

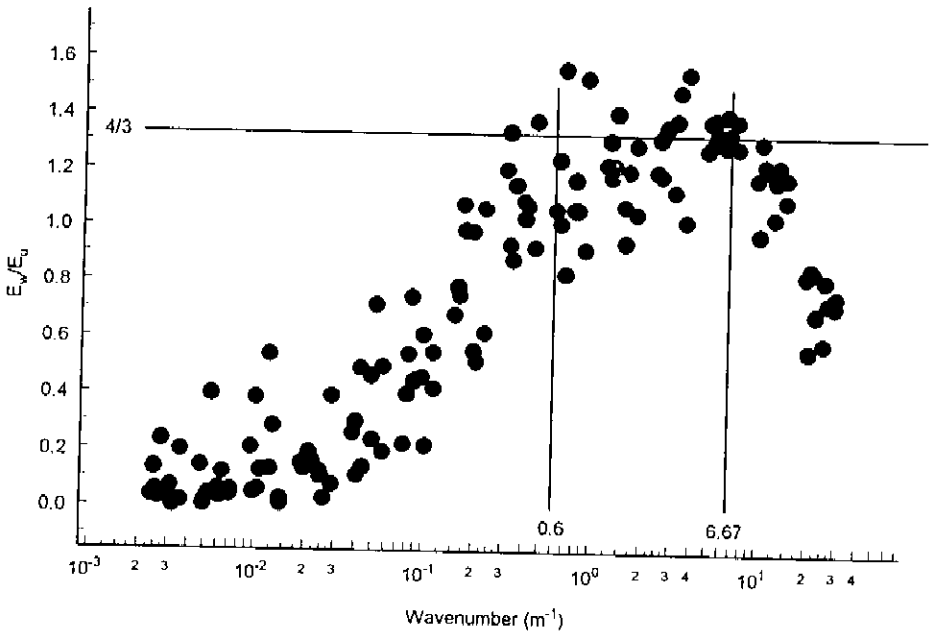

Figure 3. The ratio of the vertical velocity spectral density to the streamwise velocity spectral density for the files used in the data analysis. The local isotropy value of 4/3 is marked by a horizontal line.

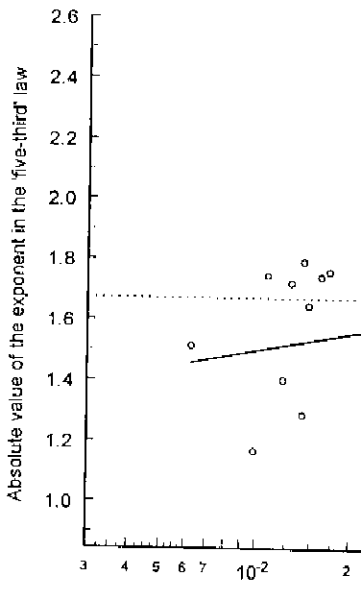

Figure 4. Absolute value of the wavenu variance of longitudinal velocities using

different variance values resulting from different 20 minute measurements in one graph.

To make certain that the wavelet spectra calculated from relatively small windows do not bring unwanted spurious effects in determining the slopes, the average of the 288 slope values for the 9 data set, 20 minute each, was calculated in order to check whether it was the same as when the slope calculation was carried out using the entire 20 minute data in one window and getting only 1 wavelet spectrum for each 20 minute data instead of the 32 different wavelet spectra for the different windows. In both cases, slope calculations were limited to wavenumbers being in the interval $\pi z^{-1} < k \leq d_{sl}^{-1}$. For the data analyzed in this study, the difference between the two slope values was less than 0.5%, indicating that the average slope of the wavelet spectrum in the inertial subrange scale is indeed $-5/3$.

5. Results and Discussion

The data analysis can be summarized as:

1. Normalization (subtracting the mean and dividing by the standard deviation) of each 20 minute data file of longitudinal and vertical velocities.
2. Transformation of each normalized 20 minute measurements using the Daubechies-4 wavelet basis function.
3. Calculation of the slope of t for each data window consis data files (32 windows per fi
4. Plot sl versus the variance fc

Results of the analysis of slc 4 and 5 for the longitudinal and that the slope of the wavelet spe the signal inside the window, the in each window. As the value c a magnitude of 1.5 to a magnitu variance. A summary for the line For both velocity components the of the signal's variance is statist 0.0005 for the two-tailed t-test fo

One can conclude, based on events (high value of variance) th characterized by low values of result is similar to that of Hagelb 'weak turbulence regimes' the sl also claimed that at the same tin the 'structure containing part' of t

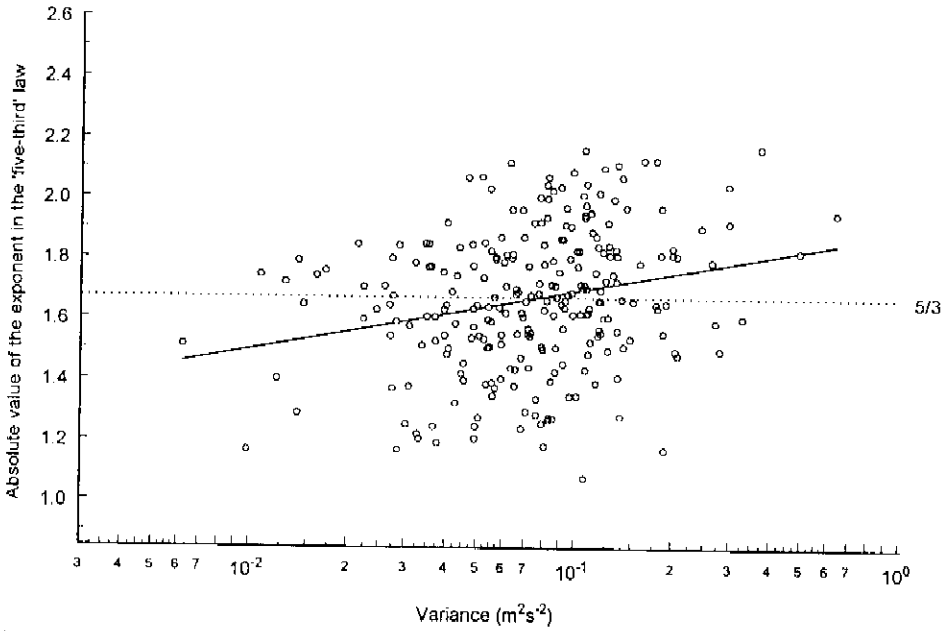

Figure 4. Absolute value of the wavenumber exponent in Kolmogorov's 'five-third' law vs. the local variance of longitudinal velocities using a window length of 2,048 data points.

3. Calculation of the slope of the local spectrum sl using (12), and the variance for each data window consisting of 2,048 data points for each of the 20 minute data files (32 windows per file).
4. Plot sl versus the variance for the two velocity components.

Results of the analysis of slope (sl) versus variance are displayed in Figure 4 and 5 for the longitudinal and vertical velocities, respectively. It can be seen that the slope of the wavelet spectra is statistically dependent on the variance of the signal inside the window, the value characterizing the extent of intermittency in each window. As the value of the variance grows, the slope increases from a magnitude of 1.5 to a magnitude of 1.8. Note the logarithmic scaling for the variance. A summary for the linear regression statistics can be found in Table II. For both velocity components the linear relationship between sl and the logarithm of the signal's variance is statistically significant even at a confidence level of 0.0005 for the two-tailed t-test for the linear regression slope parameter.

One can conclude, based on Figures 4 and 5, that in regions of intermittent events (high value of variance) the energy spectrum is steeper than that of regions characterized by low values of intermittency, which have flatter spectra. This result is similar to that of Hagelberg and Gamage (1994), who found that during 'weak turbulence regimes' the slope of the spectrum is flatter than $-5/3$. They also claimed that at the same time a spectrum with a slope of $-5/3$ exists for the 'structure containing part' of the signal. It is not clear though, whether in their

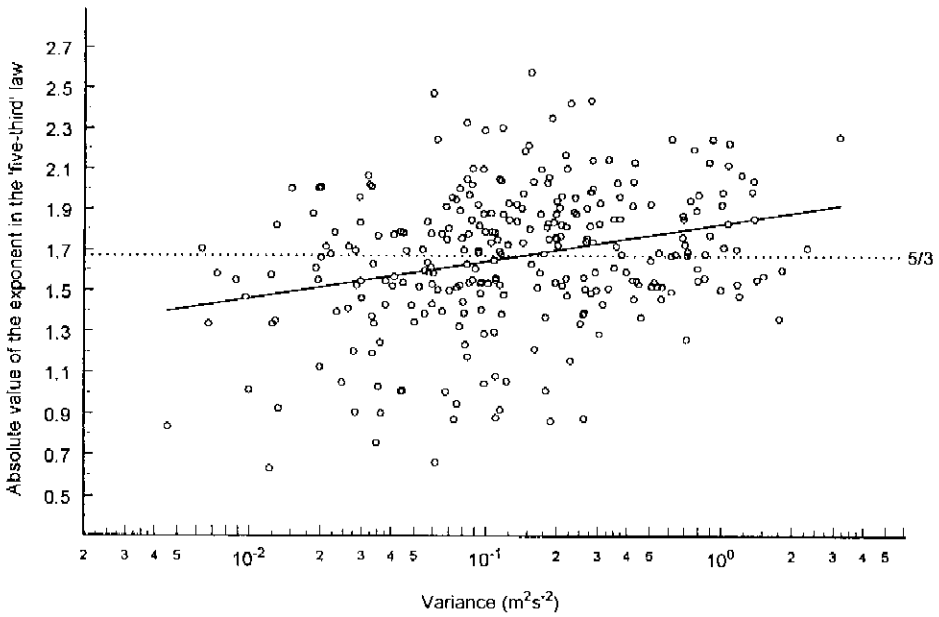

Figure 5. Absolute value of the wavenumber exponent in Kolmogorov's 'five-third' law vs the local variance of vertical velocities using a window length of 2,048 data points.

Table II

Summary of the linear regression statistics for the model $E(k) = A \ln(variance) + B$. R^2 is the coefficient of determination, S $(= (SSE/(n-2))^{1/2}$, where SSE is the error sum of squares, n is the number of observations) is the standard deviation of error, t is the t-ratio of the 2-tailed test for null hypothesis H_0: $A = 0$; t_{cr} is the critical value of the t-distribution for level $\alpha = 0.0005$; n is the number of points

Velocity component	Slope A	Intercept B	R^2	S	t	t_{cr}	n
Longitudinal	0.084	1.887	0.064	0.224	4.30	3.36	288
Vertical	0.079	1.826	0.085	0.326	5.18	3.36	288

study these findings were limited only to the inertial subrange or represent a broader scale.

Many authors argue that intermittent coherent events (or large eddies), which transfer energy to small scales (Yakhot *et al.*, 1989; Chorin, 1982; Lesieur, 1987) due to the sharp gradients and vorticity accumulation present at the edges of these structures, will result in an overall slope of the spectrum flatter than $-5/3$. For example, Yakhot *et al.* (1989), used Renormalization Group Theory (RNG) to show that the non-local nature of the energy cascade results in slopes flatter than $-5/3$. However, the picture presented in this study suggests the notion that quiescent regions with flatter spectra alternate with active regions (connected to intermittent

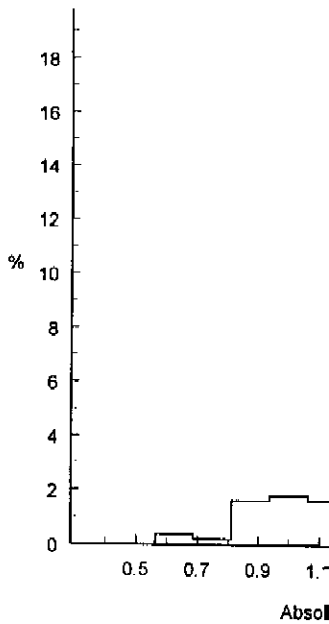

Figure 6. Histogram of the absolute v
law when data from Figures 4 and 5

events) expressing steeper spe
slope of $-5/3$ (Figure 6).

Discrete orthonormal wavelet
lence flow analysis. Due to t
space, wavelet decomposition
lent flows with concentrated r
in the energy distribution in sp
transforms, which make it pos
preserve information in the phy
for characterizing the relations
a measure (local variance of th
atmospheric boundary-layer fl
affects the slope of the local wa
slope of the local wavelet spec
while in regions of strong inte
steeper slope than $-5/3$. Howe
slope of $-5/3$ is retained as th

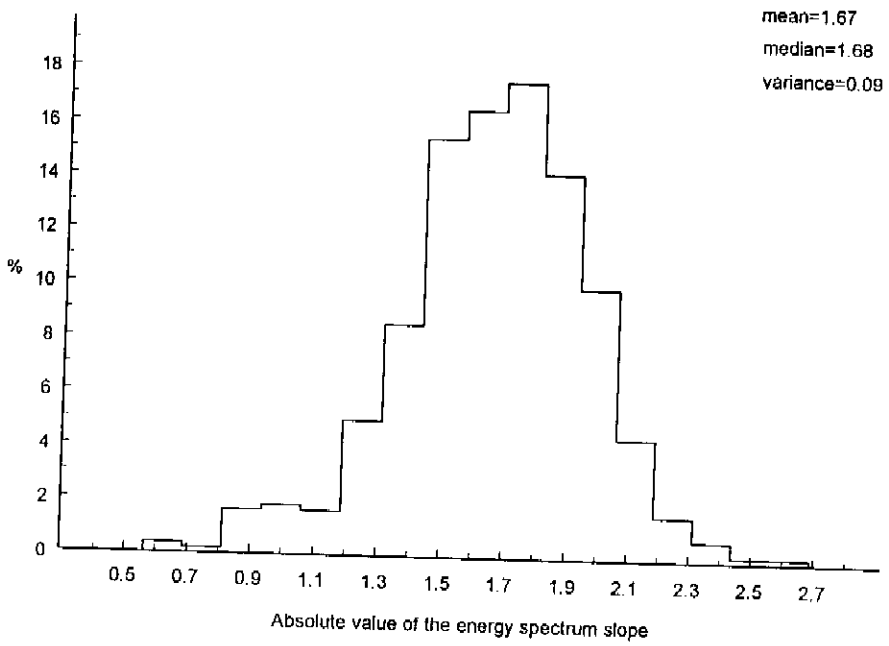

Figure 6. Histogram of the absolute values of the wavenumber exponent in Kolmogorov's 'five-third' law when data from Figures 4 and 5 are combined.

events) expressing steeper spectra than $-5/3$, thus resulting in an overall spectrum slope of $-5/3$ (Figure 6).

6. Conclusions

Discrete orthonormal wavelet decomposition was applied for intermittent turbulence flow analysis. Due to the local nature of wavelet transforms in physical space, wavelet decomposition is appropriate for characterizing intermittent turbulent flows with concentrated regions of sharp gradients. These non-uniformities in the energy distribution in space at various wavenumbers are suited for wavelet transforms, which make it possible to transform time series of turbulent flow and preserve information in the physical and wave space. This analysis was carried out for characterizing the relationship between the slope of local wavelet spectra and a measure (local variance of the signal) of local intermittency in highly turbulent atmospheric boundary-layer flow. This study concludes that local intermittency affects the slope of the local wavelet spectra. In regions of weak intermittency the slope of the local wavelet spectrum for the inertial subrange is flatter than $-5/3$, while in regions of strong intermittent events the spectrum exhibits a somewhat steeper slope than $-5/3$. However, when averaging the numerous local spectra, a slope of $-5/3$ is retained as the overall slope for the (non-local) spectrum.

Acknowledgements

The authors gratefully acknowledge the support of the National Science Foundation (EAR-93-04331) and the INCOR (Los Alamos – UCD) grant.

Appendix

The scale R_m in the wavelet transform can be expressed as $2^m dy$, where dy is the length of the sampling interval in metres. The corresponding wavenumber is $k_m = 2\pi/R_m$. Δk_m, the change in wavenumber with respect to the discrete change in scale, m ($m = 1, 2, \ldots, M = \log_2(N)$), can be approximated with Taylor's formula, when discarding higher than third-order terms as

$$\Delta k_m \sim k'_m \Delta m + \frac{1}{2!} k''_m (\Delta m)^2 + \frac{1}{3!} k'''_m (\Delta m)^3 + \cdots . \tag{A.1}$$

where k'_m, k''_m, k'''_m are the first, second and third derivatives of k_m with respect to m, Δm is the change in adjacent discrete scales, consequently, $\Delta m = 1$ always. Applying derivation and stopping after the first term in the expansion, Δk_m ($\sim k'_m$) is equal to $2\pi \ln(2)/2^m dy$ (see Meneveau, 1991a; Katul *et al.*, 1994).

However, there is no need to stop in the expansion after the first term when deriving Δk_m, instead one should retain the second and third terms for the following reasons. The first term in the expansion yields $\ln(2) k_m$ ($= 0.6931 k_m$), the second term in the expansion yields $0.2402 k_m$, while the third term gives a mere $0.0555 k_m$. If these terms are summed up, one gets $0.9888 k_m$, a value very close to 1 as the multiplier of k_m. Thus Δk_m can be expressed as

$$\begin{aligned} \Delta k_m &= \frac{2\pi}{2^m dy} \left[\ln(2) + \frac{\ln(2)^2}{2} + \frac{\ln(2)^3}{6} + \cdots \right] \\ &= 0.6931\, k_m + 0.2402\, k_m + 0.0555\, k_m + \cdots \sim k_m . \end{aligned} \tag{A.2}$$

One does not even need to use an expansion, since Δk_m can be derived directly, the following way:

$$\begin{aligned} \Delta k_m &= k_{m+1} - k_m = \frac{2\pi}{2^{m-1} dy} - \frac{2\pi}{2^m dy} = \frac{2\pi}{2^{m-1} dy} \left(1 - \frac{1}{2} \right) \\ &= \frac{2\pi}{2^m dy} = k_m . \end{aligned} \tag{A.3}$$

Thus Equation (10) is proved in two different ways.

Albertson, J. D., Kiely, G., Parlange, M
Rate of Turbulent Kinetic Energy
submitted to *J. Geophys. Res.*
Anselmet, F., Gagne, Y., Hopfinger, E.
Functions in Turbulent Shear Flows
Argoul, F., Arneodo, A., Grasseau, G.,
Analysis of Turbulence Reveals the
51–53.
Bacry, E., Arneodo, A., Frisch, U., Gag
Developed Turbulence Data and M
Lesieur (eds.), *Turbulence and Coh*
Chorin, A. J.: 1982, 'The Evolution of
Chui, C. K.: 1992, *An Introduction to W*
Cohen, L.: 1995, *Time-Frequency Anal*
Daubechies, I.: 1988, 'Orthonormal Ba
Math. **XLI**, 909–996.
Daubechies, I.: 1992, *Ten Lectures on W*
Mathematics, S.I.A.M., **61**, 357 pp.
Everson, R., Sirovich, L. and Sreenivasa
Lett. A **145**, 314–322.
Farge, M.: 1992a, 'Wavelet Transforms
24, 395–457.
Farge, M.: 1992b, 'The Continuous Wa
M. B. Ruskai, G. Beylkin, R. Coifm
Wavelets and their Applications, Jo
Friehe, C. A.: 1986, 'Fine-Scale Measu
spheric Surface Layer', in: D. Lensc
ican Meteorological Society, 269 pp
Gamage, N. K. K. and Blumen, W.: 199
Fourier, and Empirical Orthogonal
Gamage, N. K. K. and Hagelberg, C.: 1
Coherent Events using Localized T
Gao, L. and Li, B. L.: 1993, 'Wavelet
Interface', *J. Appl. Meteorol.* **32**, 17
Grossmann, A. and Morlet, J.: 1984,
Wavelets of Constant Shape', *SIAM*
Grossmann, A. and Morlet, J.: 1985, 'D
and Related Transforms', in: L. Stre
Vol. 1, World Scientific, 338 pp.
Hagelberg, C. R. and Gamage, N. K. K.
positions to Intermittent Turbulenc
(eds.), *Wavelet Transforms in Geop*
Chui, series editor, Academic Press.
Kaimal, J. C. and Finnigan, J. J.: 1994, *A*
289 pp.
Katul, G. G. and Parlange, M. B.: 19
Turbulence', *J. Atmos. Sci.* **51**(15),
Katul, G. G., Parlange, M. B. and Chu, C
Statistics in Atmospheric Surface-L
Kolmogorov, A. N.: 1941, 'The Local S
Very Large Reynolds Numbers', *Do*
Kumar, P. and Foufoula-Georgiou, E.:
Properties of Spatial Rainfall using

References

Albertson, J. D., Kiely, G., Parlange, M. B., and Eichinger, W. E.: 1995, 'The Average Dissipation Rate of Turbulent Kinetic Energy in the Neutral and Unstable Atmospheric Surface Layer', submitted to *J. Geophys. Res.*

Anselmet, F., Gagne, Y., Hopfinger, E. J., and Antonia, R. A.: 1984, 'High Order Velocity Structure Functions in Turbulent Shear Flows', *J. Fluid Mech.* **140**(63), 63–89.

Argoul, F., Arneodo, A., Grasseau, G., Gagne, Y., Hopfinger, E. J., and Frisch, U.: 1989, 'Wavelet Analysis of Turbulence Reveals the Multifractal Nature of the Richardson Cascade', *Nature* **338**, 51–53.

Bacry, E., Arneodo, A., Frisch, U., Gagne, Y., and Hopfinger, E.: 1991, 'Wavelet Analysis of Fully Developed Turbulence Data and Measurement of Scaling Exponents', in: O. Metais and M. Lesieur (eds.), *Turbulence and Coherent Structures*, Kluwer Academic Press.

Chorin, A. J.: 1982, 'The Evolution of a Turbulent Vortex', *Commun. Math. Phys.* **83**, 517–535.

Chui, C. K.: 1992, *An Introduction to Wavelets*, Academic Press, 264 pp.

Cohen, L.: 1995, *Time-Frequency Analysis*, Prentice Hall, 299 pp.

Daubechies, I.: 1988, 'Orthonormal Bases of Compactly Supported Wavelets', *Comm. Pure Appl. Math.* **XLI**, 909–996.

Daubechies, I.: 1992, *Ten Lectures on Wavelets*, CBMS-NSF Regional Conference Series in Applied Mathematics, S.I.A.M., **61**, 357 pp.

Everson, R., Sirovich, L. and Sreenivasan, K. R.: 1990, 'Wavelet Analysis of the Turbulent Jet', *Phys. Lett. A* **145**, 314–322.

Farge, M.: 1992a, 'Wavelet Transforms and their Applications to Turbulence', *Ann. Rev. Fluid Mech.* **24**, 395–457.

Farge, M.: 1992b, 'The Continuous Wavelet Transform of Two-Dimensional Turbulent Flows', in: M. B. Ruskai, G. Beylkin, R. Coifman, I. Daubechies, S. Mallat, Y. Meyer, and L. Raphael (eds.), *Wavelets and their Applications*, Jones and Bartlett, 474 pp.

Friehe, C. A.: 1986, 'Fine-Scale Measurements of Velocity, Temperature, and Humidity in the Atmospheric Surface Layer', in: D. Lenschow (ed.), *Probing the Atmospheric Boundary Layer*, American Meteorological Society, 269 pp.

Gamage, N. K. K. and Blumen, W.: 1993, 'Comparative Analysis of Low-Level Cold Fronts: Wavelet, Fourier, and Empirical Orthogonal Function Decompositions', *Mon. Wea. Rev.* **121**, 2867–2878.

Gamage, N. K. K. and Hagelberg, C.: 1993, 'Detection and Analysis of Microfronts and Associated Coherent Events using Localized Transforms', *J. Atmos. Sci.* **50**, 750–756.

Gao, L. and Li, B. L.: 1993, 'Wavelet Analysis of Coherent Structures at the Atmosphere-Forest Interface', *J. Appl. Meteorol.* **32**, 1717–1725.

Grossmann, A. and Morlet, J.: 1984, 'Decomposition of Hardy Functions into Square Integrable Wavelets of Constant Shape', *SIAM J. Math. Anal.* **15**, 723–736.

Grossmann, A. and Morlet, J.: 1985, 'Decomposition of Functions into Wavelets of Constant Shape, and Related Transforms', in: L. Streit (ed.), *Mathematics + Physics, Lectures on Recent Results*, **Vol. 1**, World Scientific, 338 pp.

Hagelberg, C. R. and Gamage, N. K. K.: 1994, 'Application of Structure Preserving Wavelet Decompositions to Intermittent Turbulence: A Case Study', in: E. Foufoula-Georgiou and P. Kumar (eds.), *Wavelet Transforms in Geophysics, Vol. IX in Wavelet Analysis and its Applications*, C. Chui, series editor, Academic Press.

Kaimal, J. C. and Finnigan, J. J.: 1994, *Atmospheric Boundary Layer Flows*, Oxford University Press, 289 pp.

Katul, G. G. and Parlange, M. B.: 1994, 'On the Active Role of Temperature in Surface-Layer Turbulence', *J. Atmos. Sci.* **51**(15), 2181–2195.

Katul, G. G., Parlange, M. B. and Chu, C. R.: 1994, 'Intermittency, Local Isotropy, and Non-Gaussian Statistics in Atmospheric Surface-Layer Turbulence', *Phys. Fluids* **6**(7), 2480–2492.

Kolmogorov, A. N.: 1941, 'The Local Structure of Turbulence in Incompressible Viscous Fluid for Very Large Reynolds Numbers', *Dokl. Akad. Nauk. SSSR* **4**, 299–303.

Kumar, P. and Foufoula-Georgiou, E.: 1993, 'A New Look at Rainfall Fluctuations and Scaling Properties of Spatial Rainfall using Orthogonal Wavelets', *J. Appl. Meteorol.* **32**, 209–222.

Lesieur, M.: 1987, *Turbulence in Fluids*, Kluwer Academic.
Liandrat, J. and Moret-Bailly, F.: 1990, 'The Wavelet Transform: Some Applications to Fluid Mechanics and Turbulence', *Eur. J. Mech., B/Fluids* **9**, 1–19.
Lumley, J. :1965, 'Interpretation of Time Spectra Measured in High Intensity Shear Flows', *Phys. Fluids* **6**, 1056–1062.
Mahrt, L.: 1991, 'Eddy Asymmetry in the Shear Heated Boundary Layer', *J. Atmos. Sci.* **48**, 472-492.
Mahrt, L. and Howell, J. F.: 1994, 'The Influence of Coherent Structures and Microfronts on Scaling Laws using Global and Local Transforms', *J. Fluid Mech.* **260**, 247–270.
Mallat, S.: 1989a, 'A Theory for Multiresolution Signal Decomposition: The Wavelet Representation', *IEEE Trans. Pattern Analysis and Machine Intelligence* **11**, 674–693
Mallat, S.: 1989b, 'Multiresolution Approximations and Wavelet Orthonormal Bases of $L^2(R)$', *Trans. Amer. Math. Soc.* **315**, 69–87.
Meneveau, C.: 1991a, 'Analysis of Turbulence in the Orthonormal Wavelet Representation', *J. Fluid Mech.* **232**, 469–520.
Meneveau, C.: 1991b, 'Dual Spectra and Mixed Energy Cascade of Turbulence in the Wavelet Representation', *Phys. Rev. Lett.* **11**, 1450–1453.
Newland, D. E.: 1994, *Random Vibrations, Spectral and Wavelet Analysis*, Longman Scientific and Technical, 477 pp.
Powell, D. and Elderkin, C. E.: 1974, 'An Investigation of the Application of Taylor's Hypothesis to Atmospheric Boundary Layer Turbulence', *J. Atmos. Sci.* **31**, 990–1002.
Praskovsky, A. A., Foss, J. F., Kleis, S. J., and Karyakin, M. Y.: 1993, 'Fractal Properties of Isovelocity Surfaces in High Reynolds Number Laboratory Shear Flows', *Phys. Fluids A* **5**, 2038–2042.
Praskovsky, A. A. and Oncley, S.: 1994, 'Measurements of the Kolmogorov Constant and Intermittency Exponent at Very High Reynolds Numbers', *Phys. Fluids* **6**(9), 2886–2888.
Qiu, J., Paw U, K. T. and Shaw, R.: 1995, 'Pseudo-Wavelet Analysis of Turbulence Patterns in Three Vegetation Layers', *Boundary-Layer Meteorol.* **72**, 177–204.
Stull, R.: 1988, *An Introduction to Boundary Layer Meteorology*, Kluwer Academic, 666 pp.
Taylor, G. I.: 1938, 'The Spectrum of Turbulence', *Proc. Roy. Soc. A* **CLXIV**, 476–490.
Tennekes, H. and Lumley, J. L.: 1972, *A First Course in Turbulence*, The MIT Press, 300 pp.
Turner, B. J., Leclerc, M. Y., Guthier, M., Moore, K. E., Fitzjarrald, D. R.: 1994, 'Identification of Turbulence Structures Above a Forest Canopy Using a Wavelet Transform', *J. Geophys. Res.* **99D1**, 1919–1926.
Wyngaard, J. C.: 1981, 'Cup, Propeller, Vane, and Sonic Anemometer in Turbulence Research', *Ann. Rev. Fluid. Mech.* **13**, 399–407.
Wyngaard, J. C. and Clifford, S. F.: 1977, 'Taylor's Hypothesis and High-Frequency Turbulence Spectra', *J. Atmos. Sci.* **34**, 922–929.
Yakhot, V., She, Z. S. and Orszag, S. A.: 1989, 'Deviation from the Classical Kolmogorov Theory of the Inertial Range of Homogeneous Turbulence', *Phys. Fluids A* **1**, 289–293.
Yamada, M. and Ohkitani, M.: 1990, 'Orthonormal Expansion and its Application to Turbulence', *Prog. Theor. Phys.: Progress Letters* **86**, 819–823.
Yamada, M. and Ohkitani, M.: 1991a, 'Orthonormal Wavelet Analysis of Turbulence', *Fluid Dyn. Res.* **8**, 101–115.
Yamada, M. and Ohkitani, M.: 1991b, 'An Identification of Energy Cascade in Turbulence by Orthonormal Wavelet Analysis', *Prog. Theor. Phys.* **86**, 799–815.

OBSERVATIONS OF ATM
EVOLUTION ABOVE THE

V. N. KUDRYAVTSEV, S. A. GRODS
Marine Hydrophysical Institute, Ukra

(Received in fin

Abstract. Ship borne measurements of atmo
temperature and radar signals are analyzed to
Gulf Stream temperature frontal zone. It was
speed and air temperature are well correlated
variations. These effects are accompanied by
identified from microwave backscatter.

For steady atmospheric conditions the
km, demonstrating positive radar signal cor
surrounding Sargasso sea and shelf water ar
effect of spatial inhomogeneity by introduci
observations. The model is able to reproduce

1. I

Effects of the atmospheric boundary
temperature fronts were observed in
et al., 1980; Mitnik *et al.*, 1989; Li
showed that spatial inhomogeneitie
changes of ABL stability accompani
above a cold front and intensificatic
and air temperature profiles and spa
fluxes. The latter is supported by th
over fronts observed in aircraft expe
Weissman *et al.*, 1994) and revealed f
et al., 1993, Beal *et al.*, in press]. Kel
must be taken into account in scatte

Johannessen *et al.* (1991) liste
boundary-layer stability) among th
late radar signals. Close correspond
the Gulf Stream area and quasi synch
demonstrated by Johannessen *et al.* (
appear as a significant element of oc
their radar observation is of great im

This paper presents the results
above an ocean front performed in

Boundary-Layer Meteorology **79:** 51–82, I